

Sufficient conditions for the additivity of stall forces generated by multiple filaments or motors

Tripti Bameta[‡]

UM-DAE Center for Excellence in Basic Sciences, University of Mumbai,
Vidhyanagari Campus, Mumbai-400098, India.

E-mail: tripti.bameta@cbs.ac.in

Dipjyoti Das[‡]

Department of Molecular, Cellular and Developmental Biology, Yale University, 219
Prospect Street, P.O. Box 27391, New Haven, CT 06511, USA

E-mail: dipjyoti.das@yale.edu

Dibyendu Das

Department of Physics, Indian Institute of Technology, Bombay, Powai, Mumbai-400
076, India

E-mail: dibyendu@phy.iitb.ac.in

Ranjith Padinhateeri

Department of Biosciences and Bioengineering, Indian Institute of Technology
Bombay, Powai, Mumbai-400 076, India

E-mail: ranjithp@iitb.ac.in

Mandar M. Inamdar

Department of Civil Engineering, Indian Institute of Technology, Bombay, Powai,
Mumbai-400 076, India

E-mail: minamdar@iitb.ac.in

Abstract. Molecular motors and cytoskeletal filaments mostly work collectively under opposing forces. This opposing force may be due to cargo carried by motors, or resistance coming from cell membrane pressing against the cytoskeletal filaments. Certain recent studies have shown that the collective maximum force (stall force) generated by multiple cytoskeletal filaments or molecular motors may not always be just a simple sum of stall force for individual filaments or motors. To understand this phenomena of excess or deficit collective force generation, we study a broad class of models of both cytoskeletal filaments and molecular motors. We argue that the stall force generated by a group of filaments or motors is additive, i.e., the stall force of N filaments(motors) is N times the stall force of one filament (motor), when

[‡] These authors have contributed equally to the work

the system is in equilibrium at stall. Consequently, we show that this additivity typically does not hold when the system departs from equilibrium at stall. We thus present a novel and unified understanding of existing models exhibiting such non-additivity, and generalize our arguments by developing new models that demonstrate this phenomena. We also propose a quantity similar to thermodynamic efficiency to provide a simple understanding of deviation from stall-force additivity for filament and motor collectives.

1. Introduction

Molecular motors, such as kinesin, dynein and myosin, and cytoskeletal filaments, such as actin and microtubule, are abundantly present inside the cell [1]. Cytoskeletal filaments give structural stability to the cell and act as tracks along which molecular motors move and perform intra-cellular transport. Many researchers have studied the dynamics of single filaments and motors in great details using experimental, theoretical and computational tools [2, 3, 4, 5, 6, 7]. However, molecular motors and cytoskeletal filaments mostly work collectively to perform their biological tasks. For instance, dynamics of multiple actin filaments is responsible for lamellipodial dynamics during crawling of cells [1, 8]. Similarly, microtubules work collectively to bring about segregation of chromosomes during mitosis [9]. Also, many dynein motors attach to molecular cargo and generate force for the purpose of cellular transportation, whereas myosin motors work collectively to generate force in stress fibers and muscle tissues [1, 10]. Hence, study of such systems, which are involved in a wide range of biological processes, requires understanding of collective force generation by cytoskeletal filaments and motors [7, 11, 12, 13, 14, 15, 16, 17, 18].

A well known technique to investigate the dynamics of cytoskeletal filaments is to observe their growth and shrinkage kinetics against a resisting force [2]. One of the important quantities, that is typically of interest to researchers, is the maximum force generated by these filaments—the force at which the mean growth velocity of the filaments is zero—and is referred in the literature as the stall force [11, 12]. It had commonly been believed in the literature that the stall force of multiple, non-interacting, filaments, always scales linearly with the number of filaments [11, 12, 14, 19]. However, in recent studies, it has been demonstrated that, in many cases, there is either enhanced or reduced co-operativity in the maximum force generated by multiple growing filaments, i.e., the stall forces need not always scale with the number of growing filaments. For example, recent theoretical studies [15, 20] on collective dynamics of cytoskeletal filaments under a constant applied force have established that, the stall forces of individual filaments are non-additive in general. This implies that the collective stall force produced by N cytoskeletal filaments (denoted by $f_s^{(N)}$) is not a simple sum of individual stall forces of single filaments, i.e., $f_s^{(N)} \neq N f_s^{(1)}$.

Similar studies have also been done for molecular motors. The technique that is mostly used to study molecular motor involves micro size dielectric particle and optical tweezers [21]. A resisting force applied via this technique measures the force velocity response of the motor. Interestingly, the non-additivity of stall forces ($f_s^{(N)} \neq N f_s^{(1)}$) has been shown by Campàs *et al* [16] for multiple processive motors, in the presence of attractive/repulsive interactions. However, in absence of such interactions the stall forces in this model are simply additive. In another paper on collective motor dynamics, Casademunt and coworkers [17] have investigated the two state model [22] for multiple motors with soft interactions, and also demonstrated that the motors can produce enhanced co-operativity in stall force generation. Thus, for systems like multiple

filaments or motors pushing against an obstacle, except under some special conditions obeyed by the kinetic rate constants, stall forces are now known to be non-additive in general. Hence, it would be both interesting and important to understand these special conditions for which stall forces become simply additive, and consequently get better insight into the circumstances under which the simple additivity is lost.

Although, many researchers have shown enhanced/reduced co-operativity in stall force generation by multiple motors and filaments, all the studies are highly context/model specific. In this paper, we develop a general framework to understand why/how enhanced/reduced co-operativity in collective force generation occurs in systems of multiple cytoskeletal filaments or motors—we investigate this question by studying various models for these systems. From our case studies we conclude, quite generally, that the violation of force-additivity at stall stems from the violation of the condition of *detailed balance*, i.e. departure from equilibrium.

The organization of the paper is as follows. In section 2, we present theoretical arguments to show that the force-additivity $f_s^{(N)} = Nf_s^{(1)}$ holds for simplest models for motors and filaments, which necessarily exhibit equilibrium at stall. We then proceed to investigate several non-equilibrium models of multiple filaments and motors in section 3, and explicitly show that the relationship $f_s^{(N)} \neq Nf_s^{(1)}$ is generally true when the system at stall is not in thermodynamic equilibrium. We further demonstrate that simple ideas from thermodynamics and equilibrium statistical mechanics can be utilized to get insights into this co-operative behavior, without the necessity to perform a detailed non-equilibrium calculation. In fact, we develop a thermodynamic and experimentally tractable quantity α , that is very similar to commonly used thermodynamic efficiency parameter, to predict the co-operative behavior of multiple filaments/motors. The main ideas and conclusions are rounded up in the final section 4. We argue that the non-equilibrium state of a single filament (motor) at stall is reflected in the non-additivity of stall forces when many such filaments (motors) work together. The main contribution of this paper is to investigate, for the first time to the best of our knowledge, a variety of models of multiple filament and motor dynamics, and recognise the hitherto invisible thread of thermodynamic equilibrium linking their collective behavior at stall.

2. Collective stall force for multiple cytoskeletal filaments and motors : stall forces are additive for equilibrium dynamics

Inspired by the growth of cytoskeletal filaments against cell membrane during cell migration, many researchers have studied models of cytoskeletal filament growth and shrinkage through addition/removal of monomers against a constant applied load [11, 12, 15, 23, 24, 25]. Similar to the filaments, molecular motors also work against load and have been modelled by many researchers [16, 17, 18, 26, 27]. Many of these filament and motor models are mathematically very similar. However, a key difference between filaments and motors is that the motors move on a one-dimensional track and therefore cannot overtake each other (Fig. 1b), while in an assembly of multiple parallel

filaments, the filament tips do overtake each other (Fig. 1a). In other words, the motors follow sequential motion while the filaments follow parallel motion. Yet, we may discuss the two problems of filaments and motors using a common simple picture as follows. Single filament grows/shrinks by addition/removal of subunits of size d with rates $u(f)$ and $w(f)$, respectively (see Fig. 1a), under a constant applied force f . Similarly, a motor moves forward/backward by a single step on a one-dimensional track of lattice constant d , against a force f acting upon it (see Fig. 1b). The forward and backward hopping rates of the motor under force are $u(f)$ and $w(f)$, respectively. Note that in this paper we measure force in the units of $k_B T/d$, where k_B is the Boltzmann constant, T is the temperature, and d is the subunit (lattice) size for filament (motor), which can be taken as unity without losing generality. Motors follow mutual exclusion, i.e., the occupancy of any lattice site, at any instant, can be either 1 or 0. On the other hand, in the case of filaments, any number of filaments can be of the same length. Let us denote the polymerization-rate (forward-hopping-rate) and depolymerization-rate (backward-hopping-rate) for filaments (motors) to be u and w , respectively, in the absence of any force ($u > w$ in general). In the presence of a constant force f , the polymerization rates (forward-hopping-rate) decreases, and depolymerization-rate (backward-hopping-rate) increases according to the following rules: $u(f) = ue^{-f\delta}$ and $w(f) = we^{f(1-\delta)}$. Here, the parameter $\delta \in [0, 1]$ is commonly known as force distribution factor [12]. Note that polymerization and depolymerization (or forward and backward hopping) can be viewed as barrier crossing processes from a valley to an adjacent one on a free energy landscape (see Fig. 2). In such a representation, δ represents the position of the free energy barrier with respect to the free energy minima.

By applying tools of equilibrium statistical mechanics, we first show that the stall forces should be additive for multiple filaments in the simplest model, where only polymerization and depolymerization processes are involved (see Fig. 1c). Let us first consider a single filament at *stall* condition. By definition, the stall force is an applied force, for which the average velocity of a single filament (motor) or a system of filaments (or motors) becomes zero [12, 15, 16]. The stall force f_s^N of N filaments can also be interpreted as the maximum force generated by the filaments, and consequently $f_s^N d$ is the maximum work that can be extracted from the filaments per subunit addition. Now, consider the dynamics of a single filament under the stall force $f = f_s^{(1)}$ applied via a rigid wall (Fig. 2a). Let the wall position be x in terms of the subunit size (see Fig. 2a). Since, the external force equals the stall force, the mean velocity of the filament is zero. It is also immediately clear that the overall subunit flux in and out of the system is also zero. Since both the velocity and the particle flux for the filament is zero, it is logical to believe that the system is in thermodynamic equilibrium at stall. Hence, using equilibrium statistical mechanics we can write the probability distribution of the wall-position $P(x)$ as follows

$$P(x) = \frac{1}{Z} e^{-\beta f_s^{(1)} x} e^{\beta \epsilon x} = \frac{1}{Z} e^{-\beta (f_s^{(1)} - \epsilon) x}, \quad (1)$$

where Z is the partition function, and $\epsilon = \ln(u/w)$ is the free energy gained per subunit

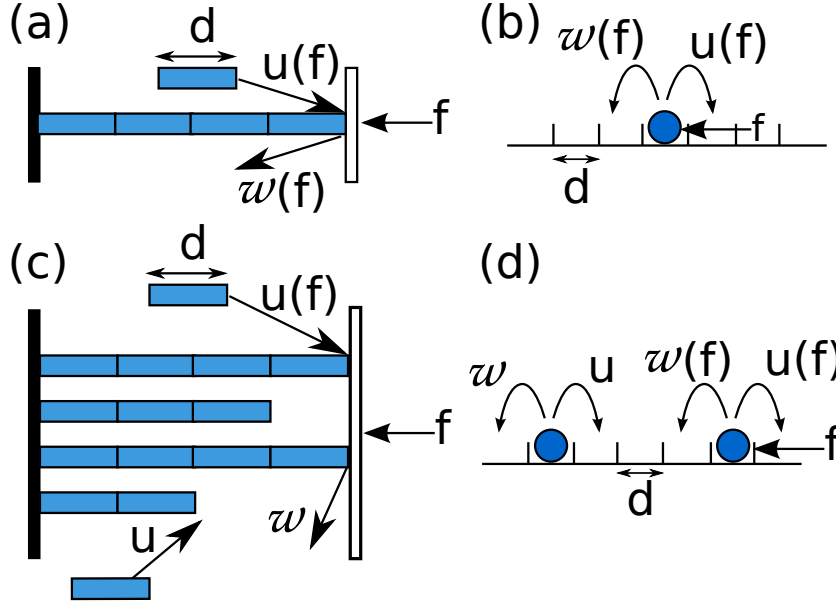


Figure 1: Biased random walk model for filaments and motors: (a) A single rigid filament growing/shrinking in presence of a resisting force f . The left wall is fixed, while the right wall is movable with a force f pressing against it. (b) A single motor moving forward/backward against a force f . (c) Multiple ($N > 1$) filaments against a wall (see [12] for a detailed study of this model). Polymerization and depolymerization rates are u and w , when the filaments are away from wall (hence force-free). Note that, when more than one filament touch the wall simultaneously depolymerization rates become force independent (w), as a single depolymerization event does not cause any wall movement. (d) Multiple motors moving on a track. Note that only leading motor bears the force f , while trailing motors are force-free.

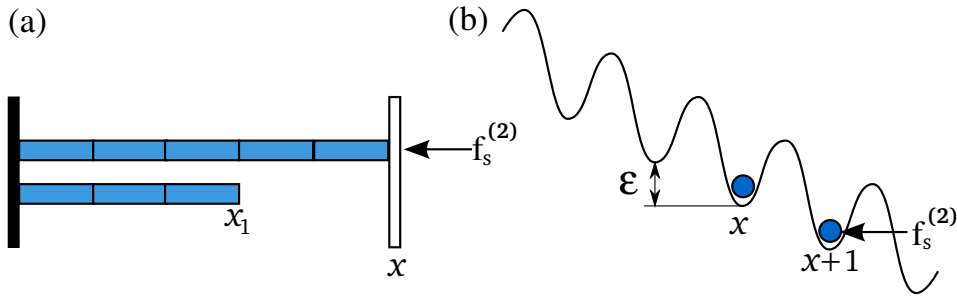


Figure 2: Filaments and motors at the corresponding stall forces: (a) Two filaments at the collective stall force $f_s^{(2)}$ undergoing simple processes of polymerization and depolymerization. (b) Two motors diffusing on a tilted free-energy landscape under the stall force $f_s^{(2)}$ applied on the leading motor.

through polymerization. Note that the term $e^{-\beta f_s^{(1)} x}$ appears as we have a Gibbs ensemble in 1-dimension with fixed external compressive force ($f_s^{(1)}$). However, this distribution $P(x)$ should be independent of x , as the stall condition should be reached

at any position x . As per Eq. 1, this implies that $f_s^{(1)} = \epsilon = \ln(u/w)$; same answer that is obtained from a detailed kinetic calculation [12]. Next, consider a two-filament system subjected to their stall force $f_s^{(2)}$ as shown in Fig. 2a. Since the system is at stall, the mean velocity of the wall is zero, and, consequently, the mean subunit flux in and out of the system is also zero—the system is thus in thermodynamic equilibrium. Let the tip-position of the trailing filament be x_1 , which is between 0 and the wall position x . The probability distribution of the wall-position, since the system is in thermodynamic equilibrium, is:

$$P(x) = \frac{1}{Z} e^{-\beta f_s^{(2)} x} e^{\beta \epsilon x} \left(2 \sum_{x_1=0}^x e^{\beta \epsilon x_1} - e^{\beta \epsilon x} \right) \\ \sim e^{-\beta (f_s^{(2)} - 2\epsilon) x}, \quad \text{for large } x \quad (2)$$

The factor of 2 appears on the right hand side, since there could be two equally likely situations—either the top-filament or the bottom-filament can be the leader (see Fig. 2). As for a single filament at stall, $P(x)$ is expected not to depend on x , implying that $f_s^{(2)} = 2\epsilon = 2f_s^{(1)}$. This argument can be easily extended to $N > 2$, and thus $f_s^{(N)} = Nf_s^{(1)}$ for this simple model. Arguments, based on detailed balance criterion, have also been given in Refs. [11] and [13] to show similar result of $f_s^{(N)} \propto N$ for their respective models on cytoskeletal filaments. However, such a simple calculation for stall force, based on elementary statistical mechanics, for an essentially kinetic process, is provided for the first time for such models, to the best of our knowledge. As we will see in the subsequent sections, this simple argument leads to major ramifications when the system is *not in equilibrium at stall*.

We can also develop similar arguments to show the additivity of stall forces for multiple motors. The forward/backward hopping processes for motors can be viewed as random walk on a tilted free-energy landscape (see Fig.2b). In this case, x and x_1 should be interpreted as the positions of the leading and the trailing motors, respectively. The free energy “released” per unit step by going downhill on the free-energy landscape is ϵ (equivalent to the polymerization energy). For a single motor under stall force, we can write a similar equation as before (Eq. 1) for the probability distribution of the leading motor’s position, $P(x)$, by recognizing the system to be in equilibrium at stall. However, for two motors at stall, the probability distribution of the leader’s position is somewhat different from the previous case of the filaments, as there is no overtaking in the case of motors—the distribution is:

$$P(x) = \frac{1}{Z} e^{-\beta f_s^{(2)} x} e^{\beta \epsilon x} \left(\sum_{x_1=0}^{x-1} e^{\beta \epsilon x_1} \right) \\ \sim e^{-\beta (f_s^{(2)} - 2\epsilon) x}, \text{ for large } x \quad (3)$$

If we again use the logic that $P(x)$ should be independent of x , we get back the force additivity : $f_s^{(2)} = 2\epsilon = 2f_s^{(1)}$. This argument hinges on the recognition that, the stall condition for this simple model is equivalent to thermodynamic equilibrium, which may not be true in many biological situations. As shown in the next sections,

the breakdown of thermodynamic equilibrium at stall for more complex models have interesting implications.

3. Stall forces are non-additive for biologically relevant non-equilibrium models

In this section, we present several case studies to show that the force inequality ($f_s^{(N)} \neq N f_s^{(1)}$) is true in general for stall dynamics departing from equilibrium—however, for certain combination of kinetic rates the relationship $f_s^{(N)} = N f_s^{(1)}$ indeed holds. We begin by analyzing various models of cytoskeletal filaments.

3.1. Random hydrolysis model for multiple cytoskeletal filaments

In cytoskeletal filaments (such as, microtubules and actin filaments), subunits are typically bound to ATP/GTP molecules. When they are connected to form cytoskeletal filaments, these molecules release phosphate and convert their ATP/GTP to ADP/GDP in a process known as ATP/GTP hydrolysis [10, 1]. The ADP/GDP-bound monomers have much higher depolymerization rates compared to ATP/GTP-bound monomers. Due to this heterogeneity the cytoskeletal filaments exhibit interesting dynamical properties. In literature, the dynamics of the cytoskeletal filaments have been theoretically studied by many researchers using the “random hydrolysis” model [28, 29, 30, 31, 32]. Here, we focus on the model discussed in Refs. [15, 30]. In Fig. 3, we show multiple filaments undergoing random hydrolysis and growing against a wall held by a constant opposing force f . In the model, each monomer can be in two states: T (ATP/GTP-bound), and D (ADP/GDP-bound). Only T monomers bind to the filaments with a rate $u(f) = ue^f$ (next to the wall) or u (away from the wall). The rate u is proportional to the concentration (c) of T monomers, and can be written as $u = k_0 c$. The depolymerization occurs with a rate w_T if the tip-monomer is T, and w_D if it is D. For simplicity we assume that there is no force dependence on the off-rates w_T and w_D (i.e. $\delta = 1$). Hydrolysis (T to D conversion) happens on any T subunit randomly in space with a rate r . Note that the conversion T→D is irreversible, as it is not balanced by a reverse conversion, which makes the dynamics inherently *non-equilibrium*. The exact analytical result for the stall force $f_s^{(N)}$ is not known for such a detailed model even for $N = 1$. We instead exactly simulate the model by kinetic Monte-Carlo using experimentally known rates [10, 33, 34] for microtubules and actin filaments.

Before proceeding to discuss the issue of stall force additivity, let us first define a parameter, the “force deviation”:

$$\Delta^{(N)} = f_s^{(N)} - N f_s^{(1)} \quad (4)$$

This parameter represents the amount of excess/deficit of force generated by N filaments collectively, compared to N times of force generated by a single filament. So the deviation $\Delta^{(N)} \neq 0$ would imply any violation of the force equality $f_s^{(N)} = N f_s^{(1)}$.

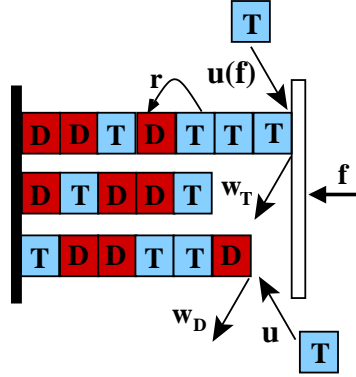


Figure 3: Random hydrolysis model with three filaments, where individual monomer switches from T to D unidirectionally and randomly. Different processes are shown by arrows.

In fact, it is recently demonstrated in Ref. [15] that the relationship $f_s^{(N)} \neq Nf_s^{(1)}$ holds, in general, for the random hydrolysis model.

We note that, the random hydrolysis model is a non-equilibrium system by construction. To understand the implications of this non-equilibrium nature, we first look at the energetics associated with the polymerization/depolymerization processes. A growing filament clearly performs work against an applied load f through polymerization. The work done for addition of one subunit to the filament is simply fd , where we can take subunit-size $d = 1$ without losing any generality. At the stall force $f = f_s^{(1)}$ (i.e. when the average filament velocity $v = 0$), the filament delivers the maximum work $W_{\text{poly}}^{\text{max}} = f_s^{(1)}$. The free energy input to the filament in order to do this work is provided by polymerisation and can be written as $F_{\text{poly}} = \ln(u/w_T)$, per subunit addition. Note that D monomers do not polymerize, and hence there is no contribution in F_{poly} due to D monomers. Finally we define the following quantity for a single filament

$$\alpha = F_{\text{poly}} - W_{\text{poly}}^{\text{max}} = \ln(u/w_T) - f_s^{(1)} \quad (5)$$

The quantity α signifies how different is the work produced per filament as compared to the free energy input. Hence, α is analogous to the thermodynamic efficiency of the system [35]. In Fig. 4a we plot the deviation $\Delta^{(2)}$ for two microtubules, and α against the dissociation rate w_D of D monomers. Other parameters are taken from the experimental literature [10, 34] (see the caption of Fig. 4). First of all, quite interestingly, $\Delta^{(2)}$ and α are correlated in sign. This gives us a hint that the violation of force additivity has something to do with the imbalance between the work produced and free-energy input (i.e. the departure from equilibrium). However, to appreciate the interconnection between $\Delta^{(2)}$ and α we first proceed to investigate the particle fluxes of the T and D monomers.

We calculate the particle fluxes when the N -filament system is at stall (i.e. at $f = f_s^{(N)}$, when average wall velocity is zero). We perform this calculation for the

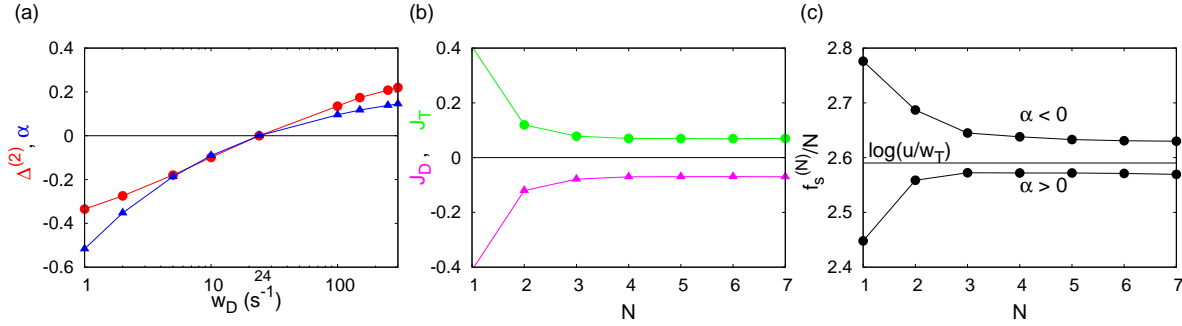


Figure 4: Random hydrolysis model for the parameter value: $k_0 = 3.2 \mu\text{M}^{-1}\text{s}^{-1}$, $c = 100\mu\text{M}$, $w_T = 24\text{s}^{-1}$, and $r = 0.2\text{s}^{-1}$. (a) $\Delta^{(2)}$ (red curve) and α (blue curve) versus w_D . Note that both α and $\Delta^{(2)}$ are zero only at $w_T = w_D$ and they are highly correlated in sign. (b) The fluxes per filament (defined in the text), at stall, for T and D monomers as a function of the filament number N for $w_D = 290\text{s}^{-1}$ ($\alpha > 0$). (c) The collective stall force per filament ($f_s^{(N)}/N$) against filament number N . For $\alpha > 0$, $w_D = 290\text{s}^{-1}$ and for $\alpha < 0$, $w_D = 5\text{s}^{-1}$.

parameter values which give $\alpha > 0$. In our simulations we separately keep track of the numbers of T and D monomers binding (or unbinding) at a filament-tip in a N -filament system. The flux J_T for T monomers is then calculated over a time window. The flux per filament is defined as the net change of T monomer numbers at any one filament-tip divided by the size of the time window. Similarly, we calculate the flux (per filament) J_D for D monomers. In Fig. 4b we show these fluxes at stall. It can be seen that although $J_T + J_D = 0$ (which is expected at stall), individually the J_T and J_D fluxes per filament are non-zero signifying the non-equilibrium nature of the dynamics. Another important point to note is that, the fluxes per filament, at stall, decreases with filament number N and tend to saturate. The dependence of particle flux (J_T or J_D) per filament with N shows a trend that is very similar to that exhibited by the deviation parameter $\Delta^{(N)}$. From this observation, we are tempted to make a hypothesis that a *non-equilibrium system with large number of filaments is closer to “equilibrium” in comparison to a single-filament system*, and as the number of filament increases the value $f_s^{(N)}$ get closer to “equilibrium” value of $\ln(u/w_T)$.

With the above hypothesis in hand, we now attempt to explain the sign correlation between $\Delta^{(2)}$ and α (Fig. 4a). First consider the case $\alpha > 0$, when the single filament system performs less work than the free-energy provided by the polymerization (for the definition of α in this case, see Eq. 5), i.e., some energy is dissipated by the filament due to the internal T \rightarrow D transitions. However, as per our hypothesis, the two-filament system is closer to equilibrium as compared to a single-filament. As a result, the two-filament system can extract more work by increasing the stall force per filament (see Fig. 4c, data shown for $\alpha > 0$)—in Fig. 4c, we clearly see that the stall force per filament $f_s^{(N)}/N$ indeed increases with N for $\alpha > 0$ (i.e. $f_s^{(N)}/N > f_s^{(1)} \forall N > 1$), and saturates near the net free-energy input (see the horizontal line corresponding to

$\ln(u/w_T)$ in Fig. 4c). This increase in stall force per filament makes $f_s^{(2)}/2 > f_s^{(1)}$ and in return gives positive $\Delta^{(2)}$. Thus, the $\alpha > 0$ case correlates with $\Delta^{(2)} > 0$. Similar arguments can be given for the other case of $\alpha < 0$ (see Fig. 4c), where the single filament system performs more work than the energy provided by polymerization. To bring the system closer to equilibrium, two-filament system decreases the stall force per filament ($f_s^{(N)}/N < f_s^{(1)}$). Hence, $\Delta^{(2)}$ is negative if $\alpha < 0$.

An interesting point to note in Fig. 4a is that both $\Delta^{(2)}$ and α are zero exactly at $w_T = w_D$. This shows that T→D switching (hydrolysis) is necessary to produce the phenomenon of non-additivity of stall forces. Note that the hydrolysis process is always non-equilibrium in nature as it is unidirectional; T→D conversion is never balanced by a reverse conversion. However, the condition $w_T = w_D$ effectively corresponds to lack of switching, since dynamically there remains no distinction between T and D subunits. The filaments cannot “sense” their distinct presence as far as the force generation is concerned. Yet, the condition $w_T = w_D$ does not imply a *true* equilibrium until we set the T→D switching rate to zero. Another way to possibly achieve equilibrium at stall is to incorporate the reverse switching (D→T) and allow polymerization of D subunits. Although these additions are biologically unrealistic, we nevertheless study such a model in the next section to explore the relevance of non-equilibrium dynamics for non-additivity of the stall forces.

3.2. A generalized random hydrolysis model

We make the random hydrolysis model (discussed in the last section 3.1) more general and symmetric by allowing (i) D → T conversion, and (ii) addition of both D and T monomers. In the model (see Fig. 5a) both T and D subunits can bind with constant rates u_T and u_D , respectively. When the filaments come in contact with the wall (see Fig. 5a), the polymerization rates modify to $u_T(f) = u_T e^{-f}$ and $u_D(f) = u_D e^{-f}$ in the presence of force f (using the load distribution factor $\delta = 1$ for simplicity). The depolymerization occurs with a rate w_T if the tip-monomer is T, or w_D if it is D. Any randomly chosen subunit inside a filament can convert either from T to D (with rate k_{TD}), or from D to T (with rate k_{DT}).

Within the general version of the random hydrolysis model, we now proceed to show that the two-way switching (T → D, and D → T) in general produces non-equilibrium dynamics that is embodied in the violation of the condition of *detailed balance* for the kinetic rates. For a single filament, as shown in Fig. 5b, we consider a loop of dynamically connected configurations. The product of clockwise and anticlockwise rates are $u_T k_{TD} w_D$ and $u_D k_{DT} w_T$, respectively. For the condition of detailed balance, i.e., equilibrium, to be reached at steady state, the two products must be equal according to the *Kolmogorov's criterion* [36, 37] (or the Wegschieder condition [38]), which leads to

$$\frac{u_T k_{TD} w_D}{w_T k_{DT} u_D} = 1. \quad (6)$$

If we fix the parameters $w_T = 2s^{-1}$, $k_{TD} = 0.3s^{-1}$, $k_{DT} = 0.4s^{-1}$, $u_D = 3s^{-1}$, and

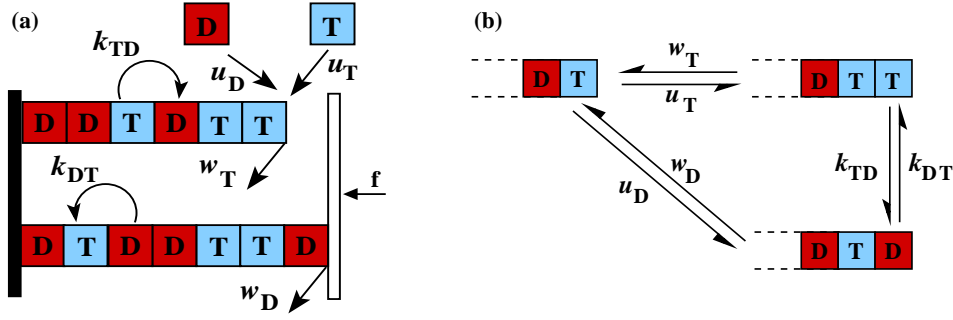


Figure 5: (a) Schematic diagram of a generalized random hydrolysis model with two-way switching (both $T \rightarrow D$, and $D \rightarrow T$). Different processes (shown in arrows) are discussed in the text. (b) Schematic depiction of a connected loop in the configuration space of a single filament, within the model.

$w_D = 1s^{-1}$, then we would have $u_T = 8s^{-1}$ from the above equilibrium condition (Eq. 6). Though this criteria is written in terms of force-free rates, it is clear that using the modified rates in the presence of resisting force would not change the Kolmogorov criterion for these rates. We now plot the deviation $\Delta^{(2)} = f_s^{(2)} - 2f_s^{(1)}$ versus u_T in Fig. 6—see the red curve (data from stochastic simulation). The plot quite interestingly shows that $\Delta^{(2)} = 0$ only at $u_T = 8s^{-1}$; otherwise it is nonzero. This clearly indicates that the phenomenon of non-additivity of stall forces is tied to the departure of the system from equilibrium. This can be compared with the arguments given in section 2, where it is shown that for cytoskeletal filament models involving no switching, and which always exhibit equilibrium at stall, the relationship $f_s^{(N)} = Nf_s^{(1)}$ holds without any restriction.

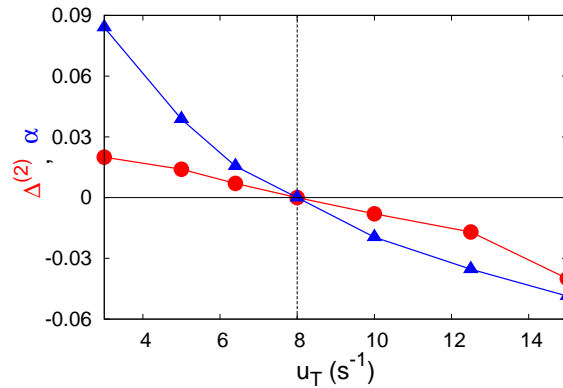


Figure 6: Deviation $\Delta^{(2)}$ versus u_T (the red curve), and α versus u_T (the blue curve), for the generalized random hydrolysis model. The parameters are: $w_T = 2s^{-1}$, $k_{TD} = 0.3s^{-1}$, $k_{DT} = 0.4s^{-1}$, $u_D = 3s^{-1}$, and $w_D = 1s^{-1}$.

We now relate the non-equilibrium effect of the force non-additivity with the imbalance between the free energy input and maximum work output (see section 3.1).

Since, in this case, at any instant filament can grow by addition of any of D or T monomer, the free energy input of the system should depend on both T and D polymerization energy. Partition function of the model is $e^{\epsilon_T} + e^{\epsilon_D}$ (using $k_B T = 1$), where ϵ_T and ϵ_D are polymerization energies provided by T and D monomers, respectively. Hence, the free energy input to the filament is $F_{\text{poly}} = \ln[e^{\epsilon_T} + e^{\epsilon_D}] = \ln[(u_T/w_T) + (u_D/w_D)]$; the maximum work done by the filament is simply $f_s^{(1)}$ (using subunit size $d = 1$). As derived in the previous section 3.1, we now define the following efficiency-like parameter for this model:

$$\alpha = F_{\text{poly}} - W_{\text{poly}}^{\text{max}} = \ln[(u_T/w_T) + (u_D/w_D)] - f_s^{(1)} \quad (7)$$

We see from Fig. 6 that both α and $\Delta^{(2)}$ are correlated in sign, and they are non-zero every where except for a single point where the system is in equilibrium at stall (according to Eq. 6). With this understanding of the relationship between the non-equilibrium dynamics and non-additivity of stall forces, we now proceed to discuss another model from literature which is studied [15] in the context of collective force generation.

3.3. A toy model for cytoskeletal filaments

In this subsection we analyze a toy model introduced in Ref. [15]. In this model (Fig. 7a), each filament can switch between two chemical states 1 and 2, with switching rates k_{12} (from 1 to 2), and k_{21} (from 2 to 1). In the states 1 and 2, the filament has distinct depolymerization rates w_1 and w_2 , respectively, and polymerization rates of u_1 and u_2 , respectively (see Fig. 7a). As an aside, we point out that this generalized model for a single filament is very similar to the switching model for microtubule dynamics introduced in Ref. [4]. If a filament bears the load (i.e. touches the wall), its polymerization rate is modified to $u_i(f) = u_i e^{-f}$ ($i = 1, 2$). For simplicity, we assume that the depolymerization rates are force independent.

Within the general version of the toy model, we first explicitly show that the stall dynamics is indeed non-equilibrium. For a single filament, as shown in Fig. 7b, we again consider a loop of connected configurations characterized by its length and state. In this case, Kolmogorov's criterion reduces to

$$\begin{aligned} u_1 k_{12} w_2 k_{21} &= k_{12} u_2 k_{21} w_1 \\ \implies \frac{u_1}{w_1} &= \frac{u_2}{w_2} \end{aligned} \quad (8)$$

Following the procedure involving microscopic Master equations, as described in Ref. [15], we analytically get the single-filament and two-filament stall forces ($f_s^{(1)}$, $f_s^{(2)}$). In Fig. 8, we plot $\Delta^{(2)}$ against u_2 (red curve) with fixed $w_1 = 0.1 s^{-1}$, $u_1 = 1 s^{-1}$, and $w_2 = 0.8 s^{-1}$ —we find that $\Delta^{(2)} \neq 0$ for all u_2 , except for $u_2 = 8 s^{-1}$ (the value corresponding to the equality in Eq. 8). This shows that the phenomenon of non-additivity of stall forces is indeed tied to the departure from equilibrium.

In the toy model, $\ln(u_i/w_i)$ is the polymerization free energy in state $i = (1, 2)$. Hence, if P_i is the probability of finding a filament in state i , then at any instant the

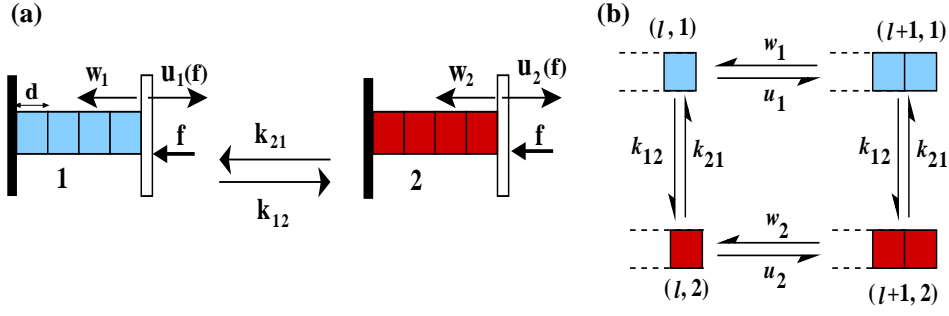


Figure 7: (a) Schematic diagram of single-filament toy model with switching between states 1 (blue) and 2 (red). Various processes are shown by arrows and corresponding rates, as discussed in the text. (b) Schematic depiction of a connected loop in the configuration space of single-filament toy model. The configurations are denoted by ordered pairs, whose first element is the instantaneous length and second element is the chemical state (1 or 2).

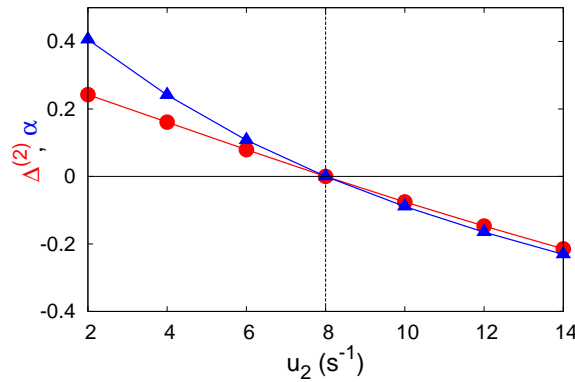


Figure 8: $\Delta^{(2)}$ (red) and α (blue) as a function of u_2 for the toy model. Parameters are $k_{12} = 0.5 \text{ s}^{-1}$, $k_{21} = 0.5 \text{ s}^{-1}$, $w_1 = 0.1 \text{ s}^{-1}$, $u_1 = 1 \text{ s}^{-1}$, $w_2 = 0.8 \text{ s}^{-1}$.

amount of free energy that is transferred from the bath of monomers to the filament upon addition of monomer type 1 or 2 is given by $F_{\text{poly}} = P_1 \ln(u_1/w_1) + P_2 \ln(u_2/w_2)$. On the other hand, the maximum amount of work done by a filament against the applied force is $W^{\text{max}} = f_s^{(1)}$ (assuming monomer size $d = 1$). Hence, as defined in the previous sections, we can again define an efficiency parameter as:

$$\alpha = F_{\text{poly}} - W^{\text{max}} = [P_1 \ln(u_1/w_1) + P_2 \ln(u_2/w_2)] - f_s^{(1)}, \quad (9)$$

where, $P_1 = k_{21}/(k_{12} + k_{21})$ and $P_2 = k_{12}/(k_{12} + k_{21})$ — this follows from the fact that the detailed balance relation $P_1 k_{12} = P_2 k_{21}$ holds at the steady state for the single-filament toy model as shown in [15] (also intuitively evident from Fig. 7a), along with the normalization condition $P_1 + P_2 = 1$. In Fig. 8, we plot α versus u_2 (blue curve). We see that $\Delta^{(2)}$ is closely coupled to α in numerical sign, and both are nonzero except at the point where equilibrium condition (Eq. 8) is satisfied.

The phenomenon of non-additivity of stall forces is not specific to cytoskeletal

filaments, even the system of multiple molecular motors can show such behavior [16]. As we describe below, the connection of this phenomenon with the non-equilibrium dynamics can also be established in systems of motors.

3.4. Model of interacting motors by Campàs et al.

A model of multiple interacting motors pushing against a load has been proposed by Campàs et al. [16] (Fig. 9a). In the model, motors walk along a 1-dimensional lattice (lattice spacing $d = 1$) and move by a single step forward (rate u) or backward (rate w). There is hard core interaction between the motors. The leading motor alone bears the load, and hence its hopping rates are modified to $u(f) = ue^{-f\delta}$, and $w(f) = we^{f(1-\delta)}$, where δ is the force distribution factor. The hopping rates change due to nearest-neighbor interactions — if a motor is adjacent to another one, its forward and backward hopping rates become \bar{u} and \bar{w} , respectively (see Fig. 9a).

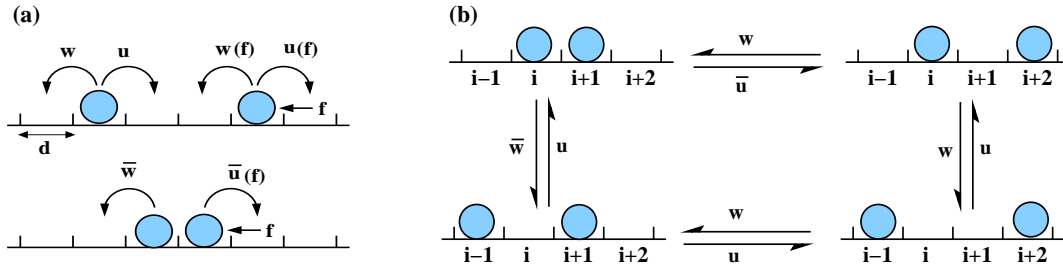


Figure 9: (a) Schematic diagram of the motor model proposed by Campàs et al. [16], where multiple interacting motors push against a cargo with a constant force f acting against their motion. Various processes are shown by arrows and discussed in the text. (b) Schematic depiction of a closed loop of dynamically connected configurations for the model shown in (a).

From analytical calculations and numerical simulations, the authors found that the stall forces are not necessarily additive. We show here that the non-additivity is a manifestation of the non-equilibrium nature of the dynamics. To show this we again apply the Kolmogorov criterion, by making a closed loop of connected configurations as shown in Fig. 9b. By equating the clockwise and counter-clockwise products of rates along the loop, we have

$$\begin{aligned} u \cdot \bar{u} \cdot w \cdot w &= \bar{w} \cdot u \cdot u \cdot w \\ \implies \frac{u}{w} &= \frac{\bar{u}}{\bar{w}} \end{aligned} \tag{10}$$

Exact analytical expressions of the single-motor stall force $f_s^{(1)} = \ln(u/w)$, and the two-motor stall force $f_s^{(2)} = \ln[(u\bar{u}/w\bar{w}) + (u/w) - (\bar{u}/\bar{w})]$ are given in [16]. If we put the equality of Eq. 10 in the expression of $f_s^{(2)}$, we clearly note that the relationship $f_s^{(2)} = 2f_s^{(1)}$ follows. We further plot (see Fig. 10) $\Delta^{(2)} = f_s^{(2)} - 2f_s^{(1)}$ versus \bar{u} , with fixed $u = 20s^{-1}$, $w = 5s^{-1}$, and $\bar{w} = 1s^{-1}$. In this case, $\bar{u} = 4s^{-1}$ corresponds to

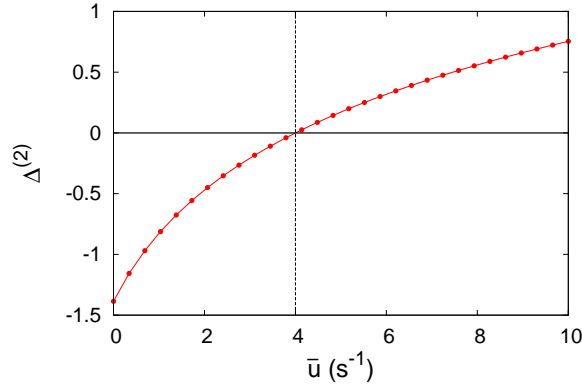


Figure 10: Deviation $\Delta^{(2)}$ versus \bar{u} within the model of Campàs et al (data obtained from the exact formula given in [16]). Parameters are specified in the text. We took the force distribution factor $\delta = 1$.

equilibrium case (Eq. 10), and we see that except for $\bar{u} = 4s^{-1}$, $\Delta^{(2)} \neq 0$ everywhere. This corroborates our hypothesis that the additivity of stall forces is closely linked with the underlying equilibrium of the system, a point not recognized in Ref. [16].

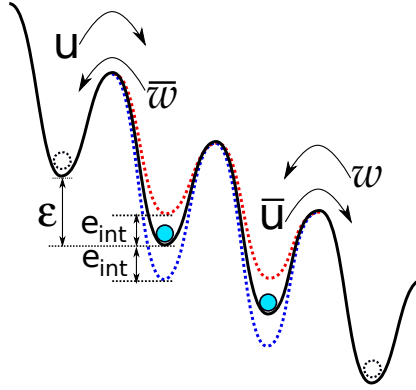


Figure 11: Motors walking on a free-energy landscape [16]. The effect of nearest neighbor interactions is shown schematically.

We can also obtain the condition of equilibrium (Eq. 10) from a simple equilibrium thermodynamic argument by considering the hopping processes of the motors on a free-energy landscape (see Fig. 11). Due to the nearest neighbor interactions, the shape of the free energy landscape alters when the motors are adjacent to each other. An attractive interaction deepens the energy wells by an amount e_{int} (dotted blue curve in Fig. 11), and makes it harder for the particles to leave the position. This reduces the forward and backward hopping rates. On the other hand, the repulsive interaction makes the potential wells shallower (dotted red curve in Fig. 11), which makes it easy for the particles to hop forward or backward. In this case, hopping rates increase from the original values. Following Fig. 11, we write following equations for the hopping rates,

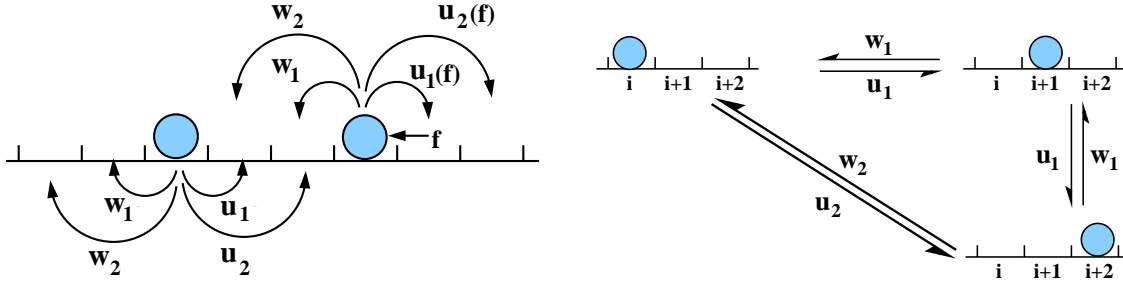


Figure 12: Multiple step size motor model: (a) Schematic diagram of the motors moving with two distinct step sizes. The kinetic processes (shown in arrows) are explained in the text. (b) A closed loop of connected configurations for the model with one motor.

when the motors are adjacent to each other:

$$\frac{u}{\bar{w}} = e^{\epsilon - e_{\text{int}}} \quad (11)$$

$$\frac{\bar{u}}{w} = e^{\epsilon + e_{\text{int}}} \quad (12)$$

For a motor which is away from the other one, $e_{\text{int}} = 0$ and we have

$$\frac{u}{w} = e^{\epsilon} \quad (13)$$

By rearranging the equations 11, 12 and 13, we get back: $\frac{u}{w} = \frac{\bar{u}}{\bar{w}}$, which is the condition in Eq. 10 and is a reflection of the equilibrium nature of stall dynamics.

3.5. A motor model with multiple step-sizes

Recently, it is shown in Refs. [6, 21] that dynein motors on a microtubule can take multiple step sizes – predominantly 24-nm and 32-nm steps. This inspired us to cast a new model of motors walking with two step sizes (see Fig. 12a). The motors walk along a 1-dimensional lattice (lattice spacing $d = 1$). A motor at a lattice site i can hop to any of the sites $i + 1$ (with rate u_1), $i + 2$ (with rate u_2), $i - 1$ (with rate w_1), and $i - 2$ (with rate w_2). The leading motor alone bears the applied force f and its forward rates are modified to $u_1(f) = u_1 e^{-f}$ and $u_2(f) = u_2 e^{-2f}$, while backward rates are assumed to be force-independent (load distribution factor $\delta = 1$). Unlike in the previous case (Section 3.4) there is no explicit attractive or repulsive interaction between the motors.

Proceeding in a similar way as described in the previous sections 3.2 and 3.3, we first of all derive the condition for equilibrium, by considering a closed loop of connected configurations as shown in Fig. 12b. Following Kolmogorov criterion we get

$$\begin{aligned} u_1^2 \cdot w_2 &= u_2 \cdot w_1^2 \\ \implies \frac{u_2}{w_2} &= \left(\frac{u_1}{w_1} \right)^2 \end{aligned} \quad (14)$$

If we take $u_1 = 80s^{-1}$, $w_1 = 8s^{-1}$, and $w_2 = 1s^{-1}$, then $u_2 = 100s^{-1}$ is the value corresponding to the equilibrium (see Eq. 14). In Fig. 13, $\Delta^{(2)}$ versus u_2 is plotted (the red curve) from our simulation results, where we indeed see that $\Delta^{(2)} = 0$ only for

$u_2 = 100s^{-1}$. Thus, one can again associate the force inequality $f_s^{(N)} \neq Nf_s^{(1)}$ to the violation of the detailed balance condition.

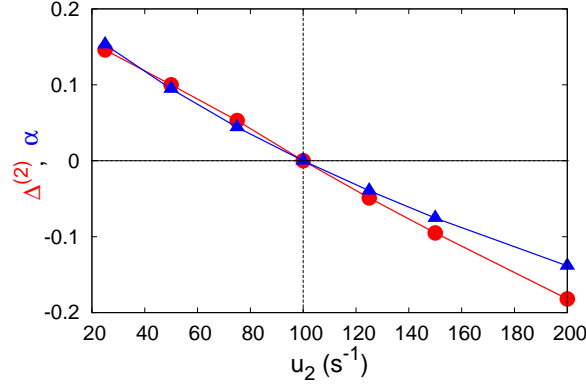


Figure 13: Deviation $\Delta^{(2)}$ versus u_2 (the red curve), and α versus u_2 (the blue curve) for the motor-model with two step sizes. The parameters are $u_1 = 80s^{-1}$, $w_1 = 8s^{-1}$, and $w_2 = 1s^{-1}$.

We would now show that the effect of force-additivity for motors is related to the underlying energetic imbalance, like the models of cytoskeletal filaments discussed in the previous sections 3.1, 3.2 and 3.3. The motor model with multiple step-size model looks conceptually similar to generalized random hydrolysis model—at any instant, a filament can grow by addition of T or D monomer in generalized random hydrolysis model, whereas in motor with multiple step-size model a motor can move forward by taking step of size d or $2d$. However, in the current model, taking a step of size d or $2d$ involves change in *work done by motor*, unlike the generalized random hydrolysis model where addition of D or T monomer leads to extraction of the same work ($f_s^{(1)}d$). Hence, for α (thermodynamic efficiency) definition, we only take into account energy imbalance that results by the motor taking step of size d . For a step of unit lattice size, we can write the free-energy supplied by ATP molecules as $F = \ln(u_1/w_1)$ and the maximum work done as $W^{\max} = f_s^{(1)}$ (considering the lattice size $d = 1$). Thus, we may define an efficiency-like quantity

$$\alpha = F - W^{\max} = \ln(u_1/w_1) - f_s^{(1)}. \quad (15)$$

We do not claim that this is a unique α which can be defined for this system. One may certainly come up with some other definition for α , for example,

$$\alpha = \frac{1}{2}(\ln \frac{u_2}{w_2} - 2f_s^{(1)}), \quad (16)$$

to quantify excess/deficit energy supplied to the system *per step*—both these definition of α (Eqs. 15 and 16) essentially capture the energy imbalance per unit step.

We plot α (from Eq. 15) and $\Delta^{(2)}$ versus u_2 in Fig. 13, and we see that both α and $\Delta^{(2)}$ are indeed correlated in sign—both are zero only for the equilibrium condition (Eq. 14). The same finding can be obtained by using Eq. 16 for α instead of Eq. 15 (data

not shown). This further strengthens our point that the phenomenon of non-additivity of stall forces is a manifestation of underlying non-equilibrium stall dynamics.

4. Discussion and conclusion

Collective force generation by filaments/motors has theoretically been studied by many researchers for various models in specific contexts [11, 12, 14, 15, 16, 17, 19, 20]. However, a broad picture explaining the cooperative effects in stall force generation is still missing. In this paper, we have addressed this problem in a more general manner. We have provided a theoretical frame-work to understand and predict the co-operative effect in the maximum force generation by multiple motors or filaments for a broad class of models. It is now known [15, 16] that the stall force of individual cytoskeletal filaments or molecular motors, when they push together against some obstacle, is not additive in general. In this paper, we have established the fact that the non-additivity of the stall forces ($f_s^{(N)} \neq Nf_s^{(1)}$) is a manifestation of the underlying non-equilibrium nature of the stall dynamics. We have first shown theoretically that the individual stall forces are expected to be additive for equilibrium dynamics. We have then compared this with various models of multiple filaments and motors, that depart from equilibrium (captured in the violation of the detailed balance condition). By using the Kolmogorov criterion [36, 37], we have systematically derived the conditions that must be obeyed by the kinetic rates if the systems are expected to be in equilibrium at stall. We have shown that when these conditions are violated, one usually gets the force inequality $f_s^{(N)} \neq Nf_s^{(1)}$. On the other hand, one gets $f_s^{(N)} = Nf_s^{(1)}$, when the balance conditions are satisfied.

Our study suggests that if the Kolmogorov criteria for kinetic rates is satisfied then one does not need a detailed non-equilibrium calculation to obtain the stall force of multiple filaments/motors. The same result can be established using a simple equilibrium statistical mechanics calculation. Moreover, even if the Kolmogorov criterion for kinetic rates is not satisfied for a problem, our thermodynamic quantity α , at least qualitatively, predicts if the co-operative effects in the stall force for multiple motors/filaments is either enhanced or decreased as one increases the number of the filaments/motors. For a class of models discussed in this paper, we clearly see a correlation between the numerical signs of α and the deviation $\Delta^{(2)}$. Although we do not have a rigorous understanding of why lack of equilibrium by-and-large leads to non-additivity of stall forces. However, we provide an intuitive argument based on our calculation of monomer flux per filament as a function of total number of filaments (see section 3.1). We have seen from our simulations that this flux per filament, which is a signature of the lack of equilibrium, decreases with the number of filaments. Hence, we make a hypothesis that the system is “pulled” towards “statistical equilibrium” as the number of filaments increase. In addition to doing detailed case studies, we provide understanding of existing results on co-operativity of multiple motors and filaments [16, 15]. To give a concrete example from the existing

literature, the results of Ref. [16] on two state motor model [17, 22] show $f_s^{(N)} \neq Nf_s^{(1)}$. Our analysis clearly indicates the same without the need for any detailed simulation or theoretical calculations. We note that, the violation of detailed balance in the transition rates between states-1 and 2, is a requirement for spontaneous motion in this two state Brownian ratchet model (see Fig. 14(a)). As a result, even for a single motor at stall, although the mean velocity flux of the motor is zero, the individual velocity fluxes in states-1 and 2 (with potentials U_1 and U_2 , respectively) for the motor are not independently zero. This non-equilibrium condition at stall for one motor is

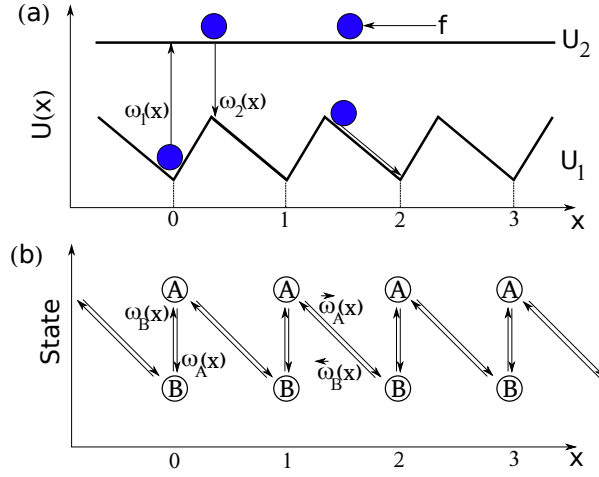


Figure 14: Schematic of the (a) continuous [22] and (b) discrete two state Brownian ratchet model [39, 40]. (a) A spontaneous motion is expected when the ratio of transition rates $\frac{\omega_1(x)}{\omega_2(x)}$ is far from equilibrium value given by detailed balance condition. (b) Discrete version of the two state ratchet model with effective transition rates $\vec{\omega}_A(x)$, $\omega_A(x)$, $\omega_B(x)$ and $\vec{\omega}_B(x)$.

manifested in the form of non-additivity of stall force in the presence of multiple, self-excluding motors, i.e., $f_s^{(N)} \neq Nf_s^{(1)}$. Interestingly, the discrete version of this two state model [39, 40], shows perfect additivity of stall forces for multiple motors with only self-inclusion interactions (see Fig. 14(b)). This results from the fact that the discrete model for a single motor can easily be mapped to a biased random walk with only one track, which implies that at stall the motor can be interpreted to be in “equilibrium.” As an interesting aside, we note that a recent experiment [41] on molecular motor dynein presumes stall force force additivity to infer the number of motors on the cargo. Our analysis, not only suggests that one has to exhibit appropriate caution due to the possible non-additivity of stall forces, but can also serve as a reasonable guide for preliminary interpretation of such experimental data before performing additional detailed analysis.

The main thesis of our paper is that if a system of molecular motors or filaments is not in equilibrium at stall we can expect co-operativity in the force generation, even in the absence of any “attractive” or “repulsive” interactions between individual components. This essentially is a new understanding, yet unreported in the literature. To establish this with reasonable certainty, we have analyzed, multiple, seemingly

disparate models which, nevertheless, exhibit a common theme of non-equilibrium stall dynamics that leads to this co-operativity.

Acknowledgments

This work is supported by DST-Inspire research grant(T. B., IFA13 PH-64), CSIR India (Dipjyoti D., JRF award no. 09/087(0572)/2009-EMR-I and Dibyendu D., no. 03(1326)/14/EMR-II.), and DBT-IYBA (M.M.I., BT/06/IYBA/2012).

References

- [1] B. Alberts, D. Bray, J. Lewis, M. Raff, K. Roberts, and J.D. Watson. *Molecular Biology of the Cell*. Garland, 4th edition, 2002.
- [2] A J Hunt and J R McIntosh. The dynamic behavior of individual microtubules associated with chromosomes in vitro. *Mol. Biol. Cell*, 9:2857–2871, 1998.
- [3] M.E. Fisher and A.B. Kolomeisky. The force exerted by a molecular motor. *PNAS*, 96:6597, 1999.
- [4] T. L. Hill and Y. Chen. Phase changes at the end of a microtubule with a GTP cap. *Proc. Natl. Acad. Sci. USA*, 81(18):5772–5776, 1984.
- [5] A.B. Kolomeisky and M.E. Fisher. Molecular motors: a theorist’s perspective. *Annu. Rev. Phys. Chem.*, 58:675, 2007.
- [6] Tripti Bameta, Ranjith Padinhateeri, and Mandar M Inamdar. Force generation and step-size fluctuations in a dynein motor. *Journal of Statistical Mechanics: Theory and Experiment*, 2013(02):P02030, 2013.
- [7] P. Ranjith, D. Lacoste, K. Mallick, and J-F. Joanny. Nonequilibrium Self-Assembly of a Filament Coupled to ATP/GTP Hydrolysis. *Biophys. J.*, 96:2146–2159, 2009.
- [8] S M Rafelski and J A Theriot. Crawling toward a unified model of cell motility: Spatial and temporal regulation of actin dynamics. *Annu. Rev. Biochem.*, 73:209–239, 2004.
- [9] J S Tirnauer, E D Salmon, and T J Mitchison. Microtubule plus-end dynamics in xenopus egg extract spindles. *Mol. Biol. Cell*, 15:1776–1784, 2004.
- [10] Jonathon Howard. *Mechanics of Motor Proteins & the Cytoskeleton*. Sinauer Associates, February 2001.
- [11] G. Sander van Doorn, Ctlin Tnase, Bela M. Mulder, and Marileen Dogterom. On the stall force for growing microtubules. *European Biophysics Journal*, 29(1):2–6, 2000.
- [12] Kostas Tsekouras, David Lacoste, Kirone Mallick, and Jean-Francois Joanny. Condensation of actin filaments pushing against a barrier. *New Journal of Physics*, 13(10):103032, 2011.
- [13] J. Krawczyk and J. Kierfeld. Stall force of polymerizing microtubules and filament bundles. *EPL (Europhysics Letters)*, 93(2):28006, 2011.
- [14] Björn Zelinski and Jan Kierfeld. Cooperative dynamics of microtubule ensembles: Polymerization forces and rescue-induced oscillations. *Phys. Rev. E*, 87:012703, Jan 2013.
- [15] Dipjyoti Das, Dibyendu Das, and Ranjith Padinhateeri. Collective force generated by multiple biofilaments can exceed the sum of forces due to individual ones. *New J. Phys.*, 16:063032, 2014.
- [16] O. Campàs, Y. Kafri, K. B. Zeldovich, J. Casademunt, and J-F. Joanny. Collective dynamics of interacting molecular motors. *Phys. Rev. Lett.*, 97:038101, Jul 2006.
- [17] Jan Brugués and Jaume Casademunt. Self-organization and cooperativity of weakly coupled molecular motors under unequal loading. *Phys. Rev. Lett.*, 102:118104, Mar 2009.
- [18] Ambarish Kunwar, Michael Vershinin, Jing Xu, and Steven P. Gross. Stepping, Strain Gating, and an Unexpected Force-Velocity Curve for Multiple-Motor-Based Transport. *Curr. Biol.*, 18(16):1173–1183, 2008.

- [19] Evgeny B. Stukalin and Anatoly B. Kolomeisky. Simple growth models of rigid multifilament biopolymers. *The Journal of Chemical Physics*, 121(2):1097–1104, 2004.
- [20] Dipjyoti Das, Dibyendu Das, and Ranjith Padinhateeri. Force-induced dynamical properties of multiple cytoskeletal filaments are distinct from that of single filaments. *PLoS One*, 9:e114014, 2014.
- [21] Roop Mallik, Brain C. Carter, Stephanie A. Lex, Stephen J. King, and steve P. Gross. Cytoplasmic dynein functions as a gear in response to load. *Nature*, 427:649–652, 2004.
- [22] Frank Jülicher, Armand Ajdari, and Jacques Prost. Modeling molecular motors. *Rev. Mod. Phys.*, 69:1269–1282, 1997.
- [23] Alex Mogilner and George Oster. Force generation by actin polymerization ii: The elastic ratchet and tethered filaments. *Biophysical Journal*, 84(3):1591 – 1605, 2003.
- [24] T L Hill. Microfilament or microtubule assembly or disassembly against a force. *Proc. Natl. Acad. Sci. USA*, 78(9):5613–5617, 1981.
- [25] C S Peskin, G M Odell, and G F Oster. Cellular motions and thermal fluctuations: the Brownian ratchet. *Biophys. J.*, 65(1):316–324, 1993.
- [26] Stefan Klumpp and Reinhard Lipowsky. Cooperative cargo transport by several molecular motors. *Proceedings of the National Academy of Sciences of the United States of America*, 102(48):17284–17289, 2005.
- [27] Melanie J. I. Mller, Stefan Klumpp, and Reinhard Lipowsky. Tug-of-war as a cooperative mechanism for bidirectional cargo transport by molecular motors. *Proceedings of the National Academy of Sciences*, 105(12):4609–4614, 2008.
- [28] Dimitrios Vavylonis, Qingbo Yang, and Ben O’Shaughnessy. Actin polymerization kinetics, cap structure, and fluctuations. *Proc. Natl. Acad. Sci. USA*, 102(24):8543–8548, 2005.
- [29] P. Ranjith, K. Mallick, J-F. Joanny, and D. Lacoste. Role of ATP hydrolysis in the Dynamics of a single actin filament. *Biophys. J.*, 98:1418–1427, 2010.
- [30] Ranjith Padinhateeri, Anatoly B Kolomeisky, and David Lacoste. Random Hydrolysis Controls the Dynamic Instability of Microtubules. *Biophys. J.*, 102:1274–1283, 2012.
- [31] Sumedha, Michael F. Hagan, and Bulbul Chakraborty. Prolonging assembly through dissociation: A self-assembly paradigm in microtubules. *Phys. Rev. E*, 83:051904, 2011.
- [32] T. Antal, P. L. Krapivsky, S. Redner, M. Mailman, and B. Chakraborty. Dynamics of an idealized model of microtubule growth and catastrophe. *Phys. Rev. E.*, 76(4):041907, 2007.
- [33] Thomas D Pollard. Rate constants for the reactions of ATP- and ADP-actin with the ends of actin filaments. *J. Cell Bio.*, 103:2747–2754, 1986.
- [34] A. Desai and T. J. Mitchison. Microtubule polymerization dynamics. *Annu. Rev. Cell. Dev. Biol.*, 13(1):83–117, 1997.
- [35] Christian Van den Broeck, Niraj Kumar, and Katja Lindenberg. Efficiency of Isothermal Molecular Machines at Maximum Power. *Phys. Rev. Lett.*, 108:210602, 2012.
- [36] A. Kolmogoroff. Zur theorie der markoffschen ketten. *Mathematische Annalen*, 112(1):155–160, 1936.
- [37] F. P. Kelly. *Reversibility and Stochastic Networks* . Wiley, Chichester, 1979.
- [38] Michael Ederer and Ernst Dieter Gilles. Thermodynamically feasible kinetic models of reaction networks. *Biophys. J.*, 92(6):1846–1857, 2007.
- [39] A. W. C. Lau, D. Lacoste, and K. Mallick. Nonequilibrium fluctuations and mechanochemical couplings of a molecular motor. *Phys. Rev. Lett.*, 99(15):158102, 2007.
- [40] D. Lacoste, A. W. C. Lau, and K. Mallick. Fluctuation theorem and large deviation function for a solvable model of a molecular motor. *Phys. Rev. E*, 78(1):011915, 2008.
- [41] ArpanK Rai, Ashim Rai, Avin J. Ramaiya, Rupam Jha, and Roop Mallik. Molecular adaptations allow dynein to generate large collective forces inside cells. *Cell*, 152(1-2):172 – 182, 2013.